Journal of Catalysis **182,** 244–256 (1999)
Article ID jcat.1998.2340, available online at http://www.idealibrary.com on IDEAL®

Solid-State Nuclear Magnetic Resonance Study of Acetone Oxime Adsorbed on CuZSM-5 and on HZSM-5

Jianjun Wu and Sarah C. Larsen[1]

Department of Chemistry, University of Iowa, Iowa City, Iowa 52242

Received September 11, 1998; revised November 11, 1998; accepted November 19, 1998

The reactions of acetone oxime, a proposed reaction intermediate for the selective catalytic reduction (SCR) of NO with propane on CuZSM-5 and on HZSM-5, have been studied with ^{13}C and ^{15}N solid-state magic-angle spinning nuclear magnetic resonance (MAS NMR). The carbon- and/or nitrogen-containing surface species, as well as the products formed under conditions of thermodynamic equilibrium, have been monitored and identified. In the absence of NO and after heating to 150–200°C, the main hydrolysis products of adsorbed acetone oxime on CuZSM-5 are acetone and hydroxylamine, while the main hydrolysis products on HZSM-5 are acetic acid and methylamine. In addition, N_2 and N_2O are formed from acetone oxime adsorbed on both HZSM-5 and CuZSM-5. In the presence of ^{15}NO, the observation of mixed-labeled ^{14}N^{15}NO and ^{15}N^{14}NO shows that new N–N bonds are formed over CuZSM-5 and HZSM-5 between two different nitrogen atoms: one from gaseous ^{15}NO molecules and the other from adsorbed acetone oxime and/or acetone oxime hydrolysis products. When ^{15}NO and unlabeled acetone oxime are reacted on CuZSM-5, the ^{14}N^{15}NO/^{15}N^{14}NO ratio is approximately 3, suggesting that the NO bond of gas-phase NO remains intact when it reacts with acetone oxime to form N_2O. It is also found that the formation of new N–N bonds from the reaction of NO and acetone oxime occurs at room temperature on CuZSM-5, but not until ∼150°C on HZSM-5. © 1999 Academic Press

Key Words: **selective catalytic reduction; solid-state nuclear magnetic resonance; CuZSM-5; HZSM-5; acetone oxime.**

INTRODUCTION

The emission of NO_x from stationary and automotive sources, such as power plants and lean-burn engines, is a major environmental pollution issue. The catalytic reduction of NO_x to N_2 is an important environmental challenge. The current commercial technology uses NH_3 for the selective catalytic reduction of NO_x (SCR-NH_3) from stationary sources (1). However, many drawbacks are associated with the use of ammonia as a reducing agent, such as the handling, storage, and slippage of ammonia, equipment corrosion, and high operating costs. For practical reasons, the selective catalytic reduction of NO_x by hydrocarbons (SCR-HC), particularly in the presence of oxygen, has attracted much interest (2–4). SCR of NO_x by hydrocarbons may also be important for applications to lean-burn gasoline and diesel engines where noble-metal three-way catalysts are not effective in the presence of excess oxygen (5).

Different hydrocarbons and various metal ion-exchanged zeolite catalysts have been evaluated for SCR-HC. Although other metal-exchanged zeolite catalysts are also active for the SCR of NO_x, CuZSM-5 has been intensively studied (6–9). Numerous studies have been conducted, with much of the research focusing on the evaluation of catalyst performance and measurement of reaction kinetics, with less emphasis on the structural characterization and spectroscopic identification of surface species. Currently, several different reaction intermediates have been proposed for the conversion from NO_x to N_2, such as an adsorbed nitrogen oxide complex NO_y ($y \geq 2$) (10–12), a carbonaceous deposit (13), oxygenated hydrocarbons (14, 15), isocyanates (16), nitrite and nitrate complexes (17), and nitro or nitroso compounds (10, 18–22).

Recently, the role of the surface nitroso complex was examined by Beutel *et al.* (10, 23). It was reported that NO reacts with alkyl radicals, which have been formed by H-abstraction and the H-abstraction is mediated by the chemisorbed NO_y complex, to form nitro- or nitroso-alkanes (10, 23, 24). The nitroso-alkanes are unstable and should immediately isomerize to form an oxime (25). Beutel *et al.* have studied the interaction of the isomerization product of nitrosopropane, ^{14}N-labeled acetone oxime, with ^{15}NO on CuZSM-5 (10). They observed the production of ^{14}N^{15}N and ^{14}N^{15}NO (and/or ^{15}N^{14}NO) by the combination of FT-IR surface studies and mass spectrometry for gas-phase analysis. The isotopic labeling studies show that N–N bonds form via interaction of gaseous NO with an adsorbed oxime complex. However, ^{14}N^{15}NO and ^{15}N^{14}NO were not distinguished in those studies.

Motivated by these previous results, we have used solid-state MAS NMR (magic-angle spinning nuclear magnetic resonance) spectroscopy to study the reactions of the proposed reaction intermediate, acetone oxime, on CuZSM-5

---

[1] To whom correspondence should be addressed. Fax: (319) 335–1270. E-mail: sarah-larsen@uiowa.edu.

0021-9517/99 $30.00

and HZSM-5. NMR is a powerful noninvasive probe that can be used to obtain valuable structural and mechanistic information about catalysts. Previous NMR studies have demonstrated numerous applications of NMR in which catalytic reactions on zeolites have been monitored and surface phenomena on supported metal catalysts have been studied (26–28). In this paper, solid-state NMR studies were initiated to investigate the interaction of adsorbed acetone oxime and its hydrolysis products with NO on CuZSM-5 and HZSM-5, which are both active for SCR-HC. Through the combination of ^{13}C and ^{15}N NMR and isotopic labeling, the carbon- and/or nitrogen-containing adsorbed surface species and/or gaseous products formed under conditions of thermodynamic equilibrium were monitored and identified.

EXPERIMENTAL

Synthesis and Characterization of Catalysts

NaZSM-5 zeolite was hydrothermally prepared by a template-free synthesis procedure (29–31). $Al(OH)_3$ 3.0 g and NaOH 6.0 g were dissolved in 250 ml of deionized water and were added slowly with stirring to 106.5 g of silica sol (Ludox 40%). Seed crystals of ZSM-5 (0.37 g) were then added to the above gel mixture to promote crystallization. The gel was transferred to Teflon-lined Parr autoclaves, placed in an oven, and heated to 453 K for 48 h. The crystallized zeolite was washed with deionized water and dried overnight at 353 K. The crystallinity of NaZSM-5 was verified by powder X-ray diffraction (XRD) on a Siemens (D5000) diffractometer. The crystal morphology and size were examined by scanning electron microscopy (SEM) on Hitachi s-4000 SEM. The elemental composition of Al and Si was determined by inductively coupled plasma/atomic emission spectroscopy (ICP/AES) using a Perkin–Elmer Plasma 400. The framework and/or nonframework aluminum and the local Si/Al distribution were characterized by ^{27}Al and ^{29}Si MAS NMR, respectively.

Copper-exchanged ZSM-5 (CuZSM-5) was prepared by a conventional ion-exchange method (31). A 200-ml aqueous solution of 0.01 M $Cu(NO_3)_2$ was added to 2 g of NaZSM-5 and the mixture was stirred for 24 h at room temperature. The product was filtered, washed with 1 liter deionized water, and finally dried in air. The content of Cu in the CuZSM-5 sample was 2.4 wt% [corresponding to 120% exchanged (2x Cu)/Al)] by ICP/AES. The XRD pattern, Si/Al ratio (see Table 1), and ^{27}Al, ^{29}Si MAS NMR of the CuZSM-5 were identical to those of the parent NaZSM-5, implying that the Cu ions were incorporated into the ZSM-5 cavities without formation of large CuO crystals in the pore structure or on the external surface of zeolite. The CuZSM-5 was degassed (1×10^{-3} Torr, 1 Torr = 133.3 Pa) prior to being used in the adsorption and reaction.

TABLE 1

Elemental Analysis Data for Zeolite Samples

Catalyst	wt% Si	wt% Al	wt% Cu	Si/Al	Cu/Al
NaZSM-5	46.7	1.76	—	25.4	—
CuZSM-5	44.8	1.70	2.4	25.3	0.60
HZSM-5	49.0	1.80	—	26.1	—

HZSM-5 catalyst was prepared by exchanging the Na^+ in NaZSM-5 with NH_4^+ which subsequently decomposed to produce NH_3 and the Brønsted site. The exchange was achieved by soaking 10 g of NaZSM-5 in 500 ml of 0.1 M NH_4NO_3 for 24 h and drying the product at 80°C for 2 h. The final step was to heat the product under vacuum (10^{-5} Torr) to 400°C over 6 h, and then to maintain this temperature for 18 h. The HZSM-5 was characterized using the procedure described above for CuZSM-5. The elemental analysis data for NaZSM-5, CuZSM-5, and HZSM-5 are shown in Table 1. Using ICP/AES, no measurable amount of impurity Fe was found in these zeolites.

Synthesis of Labeled Acetone Oxime

The ^{13}C (C-2 labeled)- and ^{15}N-labeled acetone oximes were synthesized according to procedures in the literature (32). For the synthesis of acetone [2-^{13}C]oxime, 0.5 g of hydroxylamine hydrochloride was dissolved in 2 ml of deionized water in a small beaker. [2-^{13}C]Acetone-2-^{13}C 0.75 g was added to the beaker, followed by the dropwise addition of saturated $NaHCO_3$ with stirring until the pH reached 7.0. The mixture was stirred for 3 h, and then the product was extracted with two 10-ml portions of ethyl ether. The solvent was removed by distilling and the product was recrystallized from petroleum ether. ^{15}N-labeled acetone oxime was synthesized as described above, except that the reactants were acetone and ^{15}N-labeled hydroxylamine hydrochloride. The synthesized ^{13}C- or ^{15}N-labeled acetone oxime was characterized by FT-IR and ^{1}H, ^{13}C solution-state NMR. The synthesized labeled acetone oxime products were found to be identical to the acetone oxime (ACROS) that was used as a standard.

Reagents and Materials

[2-^{13}C]Acetone (99% ^{13}C) was obtained from Isotech. [^{15}N]Hydroxylamine hydrochloride (98%+ ^{15}N), [^{15}N]methylamine hydrochloride (98%+ ^{15}N), [^{15}N]nitric oxide (98%+ ^{15}N), and [1-^{13}C]acetic acid (99% ^{13}C) were obtained from Cambridge Isotope. All of these compounds were used as purchased. Acetone oxime (98%) was obtained from Acros. Nitric oxide (C.P., 99% min) was obtained from Matheson. Acetone and petroleum ether were obtained from Fisher Scientific. Ethyl ether (GR), sodium bicarbonate (GR), and sodium hydroxide (GR) were obtained from EM Science. Hydroxylamine hydrochloride (99%), sodium isocyanate (96%), *N*-methylacetamide (99%+), methylamine (40 wt% solution in water), aluminum hydroxide hydrate ($Al(OH)_3 \cdot xH_2O$), and Ludox (40%) were obtained from Aldrich.

Preparation of Samples

CuZSM-5 or HZSM-5, typically 0.3 g, was impregnated *ex situ* with an aqueous acetone oxime solution. Samples with acetone oxime/(H or Cu) ratios of 1 : 1, 3 : 1, and 8 : 1 were prepared. Samples were also prepared by impregnation of hydroxylamine hydrochloride or methylamine hydrochloride on CuZSM-5 or HZSM-5 with a 1 : 1 loading. Another sample was also prepared with acetone adsorbed on CuZSM-5.

All the samples, preadsorbed with acetone oxime, hydroxylamine, methylamine, or acetone, were dried at room temperature to avoid decomposition, and then were loaded into glass ampoules. The glass ampoule was a modified version of a design used by Haw and co-workers (26). The glass ampoule was prepared by attaching a 6.0-mm Pyrex tube with an ∼1.5-mm neck to a vacuum valve. A small glass rod held by an aluminum disk was placed into the neck of the ampoule to ensure concentric and symmetric sealing of the ampoule. The aluminum disk had several holes in it, with the central hole to hold the glass rod and the other holes to permit the free passage of gases to the zeolite samples. The glass ampoules were outgassed *in situ* on a vacuum rack, and then nitric oxide was introduced into the ampoules on the vacuum rack by immersing the ampoule in liquid nitrogen. A torch was used to seal the ampoule. The nitric oxide introduced into the ampoules contained $1.5\text{–}3.0 \times 10^{17}$ molecules of NO. Nitric oxide was the limiting reagent when acetone oxime and NO were both added to samples of HZSM-5 or CuZSM-5. The sealed ampoules were then placed in Chemagnetics 7.5-mm (o.d.) pencil rotors for magic-angle spinning (MAS) NMR measurements. Incremental off-line heating of the samples was used and the reaction temperature was controlled by an Omega (CN-76000) programmable temperature controller.

Various samples, with the following different combinations of adsorbates on CuZSM-5 and on HZSM-5, were prepared: acetone [^{15}N]oxime, acetone [2-^{13}C]oxime, [^{15}N]hydroxylamine hydrochloride, acetone [2-^{13}C]oxime + ^{14}NO, acetone oxime + ^{15}NO, acetone [2-^{15}N]oxime + ^{14}NO, [^{15}N]hydroxylamine hydrochloride + NO, hydroxylamine hydrochloride + ^{15}NO, [^{15}N]methylamine hydrochloride + acetone, methylamine hydrochloride + ^{15}NO, [^{15}N]methylamine hydrochloride + NO, ^{15}NO only, as well as (acetone + ^{15}NO) on CuZSM-5.

NMR Spectroscopy

All the ^{27}Al, ^{29}Si, ^{13}C, and ^{15}N NMR spectra were obtained using a wide-bore Bruker MSL-300 NMR spectrometer operating at 78.205, 59.621, 75.470, and 30.425 MHz for ^{27}Al, ^{29}Si, ^{13}C, and ^{15}N, respectively. A Chemagnetics double-channel 7.5-mm pencil MAS probe was used to spin rotors loaded with the sealed samples at 4.5–5.0 kHz at the magic angle. Single-pulse direct excitation was used for ^{27}Al, ^{29}Si, and ^{15}N, with the $\pi/2$ pulse widths of 3.5, 6.0, and 7.0 μs, respectively. Recycle delay was 1 s for ^{27}Al, 10 s for ^{29}Si, and 1 s for ^{15}N. Several pulse sequences, such as cross-polarization (CP), single-pulse excitation with high-power proton decoupling, and single-pulse direct excitation were used for ^{13}C NMR signal acquisition with the following parameters: CP, contact time 1.5 ms, recycle delay 2.5 s, typical 90° pulse length 7.0 μs, single-pulse direct excitation: recycle delay 3 s, $\pi/2$ pulse length ranging from 6.0 to 8.0 μs. A line broadening of 50 Hz was used for ^{15}N spectra, and one of 10 Hz for ^{27}Al, ^{29}Si, and ^{13}C spectra. Tetramethylsilane (TMS) and 1 M $Al(NO_3)_3$ solution were used as chemical shift references for ^{29}Si and ^{27}Al, respectively. Solid adamantane mixed with KBr (28.5 ppm) and saturated $NH_4{}^{15}NO_3$ (−4 ppm) were used as external chemical shift standards for ^{13}C and ^{15}N. All the chemical shifts for ^{13}C and ^{15}N are reported relative to TMS and to CH_3NO_2, respectively. All of the NMR spectra were acquired at 25°C. ^{13}C spectra recorded with single-pulse direct excitation show a broad background signal around 110 ppm which disappears during cross-polarization experiments.

RESULTS

Decomposition of Adsorbed Acetone Oxime on HZSM-5 and on CuZSM-5

Figure 1 shows the ^{13}C CP/MAS NMR spectra acquired after a sealed sample of acetone [2-^{13}C]oxime adsorbed on HZSM-5 at 1 : 1 loading was heated from room temperature to 200°C and cooled to room temperature for data acquisition. For ^{13}C MAS spectra, both cross-polarization and single-pulse direct excitation spectra were acquired at room temperature, but only CP/MAS spectra are shown. The ^{13}C NMR peak at 172 ppm in Fig. 1a is assigned to the C-2 labeled carbon of adsorbed acetone oxime by comparison with the chemical shift for solid synthesized acetone [2-^{13}C]oxime which was measured to be 156 ppm. This peak shifted to 164 ppm when the loading of acetone [2-^{13}C]oxime was increased to 3 : 1 or 8 : 1 acetone oxime/H sites. Similar coverage dependence has been observed for carbonyl compounds, such as acetone, and is discussed in a later section (33, 34). There was no observable change in the ^{13}C CP/MAS NMR spectrum when the acetone [2-^{13}C]oxime sample was heated from room temperature to 150°C. However, after the sample was heated to 200°C

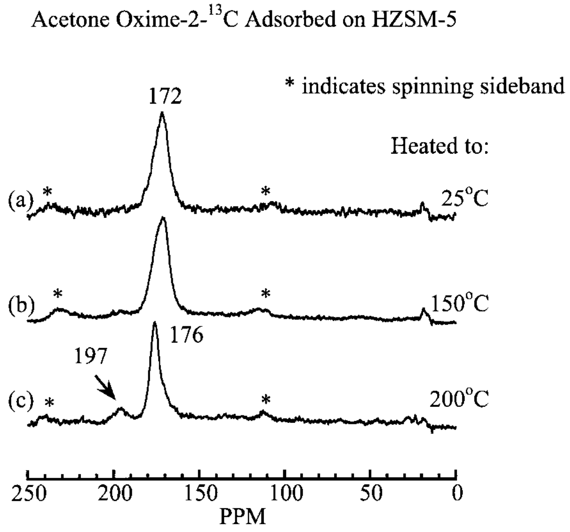

FIG. 1. ^{13}C CP/MAS NMR spectra of acetone [2-^{13}C]oxime adsorbed on HZSM-5 before and after heating to the indicated temperatures. Asterisks denote spinning sidebands. Spectra were acquired at room temperature after the sealed sample was heated to (a) 25°C, (b) 150°C, and (c) 200°C. NS (number of scans acquired) was (a) 1800, (b) 3280, and (c) 2400.

(Fig. 1c), the 172-ppm peak assigned to the C-2 carbon of acetone [2-^{13}C]oxime shifted to 176 ppm and a new peak at 197 ppm emerged. The peak at 176 ppm is assigned to the carbonyl carbon of acetic acid (33) and/or *N*-methylacetamide. In a separate experiment, the ^{13}C NMR spectra of authentic samples of *N*-methylacetamide and acetic acid both adsorbed on HZSM-5 yielded carbonyl peaks at 177 and 178 ppm, respectively. Therefore, since the peak observed at 176 ppm is broader than the 1-ppm difference in chemical shift between *N*-methylacetamide and acetic acid, it may contain contributions from both compounds. The ^{13}C NMR line at 197 ppm is assigned to *N*-methyl-2-propanimine by comparison with the NMR data for similar imines adsorbed on HZSM-5 (34, 35). *N*-methyl-2-propanimine was formed by the reaction of acetone oxime hydrolysis products, acetone and methylamine. This was confirmed in a separate experiment of the reaction of adsorbed CH_3NH_2 on HZSM-5 with [2-^{13}C]acetone in which a peak at approximately 195 ppm was observed in the ^{13}C CP/MAS experiment. In the single-pulse direct excitation ^{13}C NMR spectra of [2-^{13}C]acetone oxime, a ^{13}C NMR line at 124 ppm emerged after the sample was heated to 250°C and it is assigned to gas-phase CO_2 (26). Peak assignments are summarized in Table 2. The NMR spectra of samples heated in excess of 200°C are not shown because the decomposition or reaction of acetone oxime is complete by this temperature even though the relevant SCR temperature is ∼400°C.

^{15}N MAS NMR spectra of acetone [^{15}N]oxime adsorbed on HZSM-5 at 1 : 1 loading are presented in Fig. 2. ^{15}N

TABLE 2

Assignments of ^{13}C and ^{15}N Chemical Shifts for Chemical Species Observed in This Study

Adsorbate	δ(^{13}C-2)[a]	δ(^{15}N)[b]
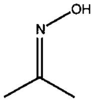	172[c] (HZSM-5) 166[c] (CuZSM-5) 156 (solid, synthesized-^{13}C)	−148[c] (HZSM-5) −102[c] (CuZSM-5) −55 (solid, synthesized ^{15}N)
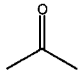	212[d] (CuZSM-5)	
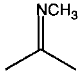	197[d] (HZSM-5) 190[d] (CuZSM-5)	−191[d] (HZSM-5)
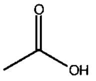	176 (HZSM-5)	
CH_3NH_2, NH_4^+		−363 to −364 (HZSM-5)
NH_2OH		−298 (HZSM-5)
N_2		−72 (HZSM-5, CuZSM-5)
N_2O		−148[e] (HZSM-5, CuZSM-5)
		−232 to −235[f] (HZSM-5, CuZSM-5

[a] Reported in ppm relative to TMS.

[b] Reported in ppm relative to CH_3NO_2.

[c] Approximately one adsorbate molecule per Brønsted acid or cation site.

[d] Adsorbate loading not known.

[e] Central nitrogen of N_2O ($N^{15}NO$).

[f] Terminal nitrogen of N_2O (^{15}NNO).

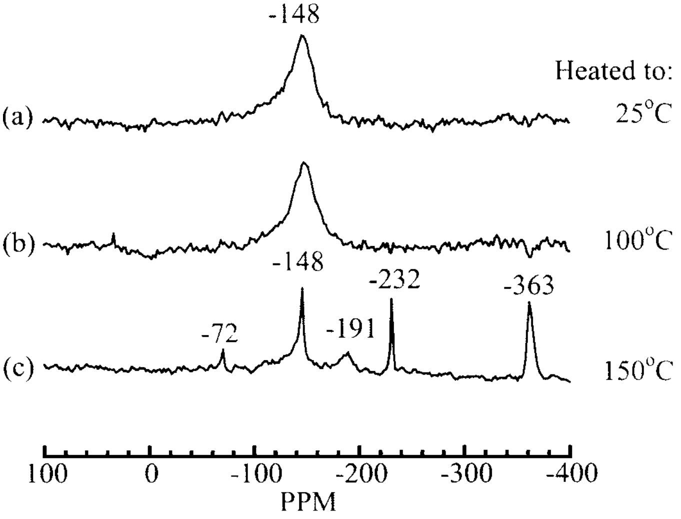

FIG. 2. ^{15}N MAS NMR of acetone [^{15}N]oxime adsorbed on HZSM-5 before and after heating to the indicated temperatures. Spectra were acquired at room temperature after the sealed sample was heated to (a) 25°C, (b) 100°C, and (c) 150°C. NS (number of scans acquired) was (a) 8400, (b) 10,600, and (c) 5500.

NMR peaks were observed at −72, −148, −191, −232, and −363 ppm. The single peak at ∼−148 ppm in Fig. 2a is assigned to acetone [^{15}N]oxime adsorbed on HZSM-5. The measured chemical shift for solid synthesized acetone [^{15}N]oxime is −55 ppm. The difference in ^{15}N chemical shifts for the solid and adsorbed acetone [^{15}N]oxime is most likely due to hydrogen bonding effects which have previously been observed for imines in solution (35, 36). When the sample was heated to 150°C and subsequently cooled for data acquisition (Fig. 2c), several new peaks appeared at −72, −148, −191, −232, and −363 ppm. The single ^{15}N peak at −72 ppm is assigned to $^{15}N_2$ and the two peaks at −148 ppm (central N) and −232 ppm (terminal N) are assigned to $^{15}N_2O$ (37). The peak at −191 ppm in the ^{15}N NMR spectrum in Fig. 2c is assigned to adsorbed *N*-methyl-2-propanimine (35). The peak at −363 ppm is assigned to methylamine or NH_4^+ (35). A separate adsorption experiment with an authentic sample of [^{15}N]methylamine on HZSM-5 yielded a peak at −361 ppm. Even though $^{15}NH_4^+$ would also produce a peak at ∼−363 ppm in the ^{15}N NMR spectrum, the peak is most likely due to methylamine according to reaction schemes that are presented in the Discussion (38).

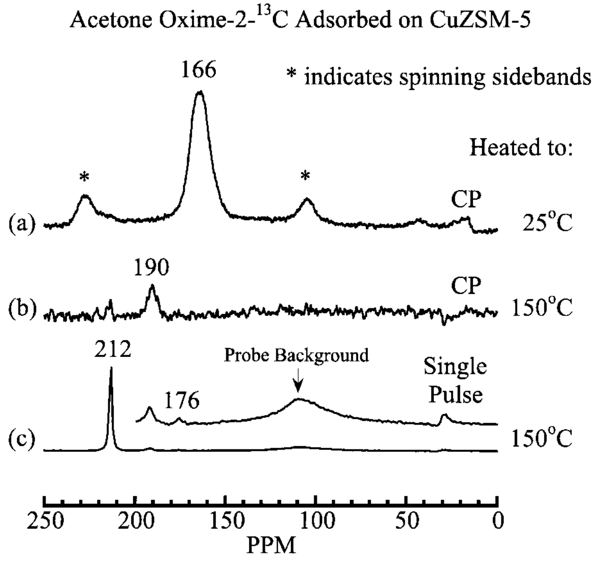

FIG. 3. ^{13}C MAS NMR spectra of acetone [2-^{13}C]oxime adsorbed on CuZSM-5. Both single-pulse excitation and cross-polarization (CP) spectra are shown. Asterisks denote spinning sidebands. Spectra were acquired at room temperature after the sealed sample was heated to (a) 25°C CP, (b) 150°C CP, and (c) 150°C single pluse. NS (number of scans acquired) was (a) 3820, (b) 1810, and (c) 5240.

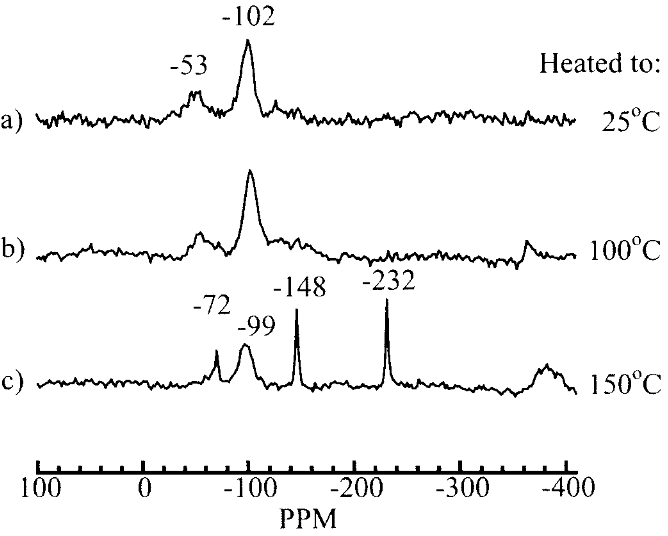

FIG. 4. ^{15}N MAS NMR spectra of the decomposition products of acetone [^{15}N]oxime adsorbed on CuZSM-5. Spectra were acquired at room temperature after the sealed sample was heated to the indicated temperatures: (a) 25°C, (b) 100°C, (c) 150°C. NS (number of scans acquired) was (a) 12,800, (b) 14,800, and (c) 6600.

The ^{13}C and ^{15}N MAS NMR spectra of adsorbed acetone [2-^{13}C]oxime and acetone [^{15}N]oxime on CuZSM-5 (1 : 1 loading) are presented in Figs. 3 and 4. The ^{13}C NMR peak at 166 ppm in Fig. 3a is assigned to the C-2 labeled carbon of adsorbed acetone oxime. This peak shifted to 162 ppm when the loading of acetone [2-^{13}C]oxime was increased to 3 : 1 or 8 : 1 acetone oxime/Cu sites. After the sealed sample was heated to 150°C and cooled to room temperature for data acquisition, ^{13}C NMR peaks were observed at 212 ppm, 190 ppm (in Figs. 3b and 3c), and 176 ppm (in Fig. 3c). These peaks are assigned to the C-2 carbons of acetone (212 ppm) (33, 34), *N*-methyl-2-propanimine (190 ppm), and acetic acid (176 ppm) (33), respectively. The peak at ∼−102 ppm in the ^{15}N NMR spectrum of acetone [^{15}N]oxime at 25°C in Fig. 4a is assigned to acetone oxime adsorbed on CuZSM-5. The peak at ∼−53 ppm is assigned to acetone [^{15}N]oxime on the external surface of the zeolite, since the chemical shift value corresponds to the chemical shift for solid acetone [^{15}N]oxime (−55 ppm vs CH_3NO_2). The presence of excess acetone [^{15}N]oxime on the external surface of the zeolite suggests that the adsorption of acetone oxime was not complete. After the sample is heated to 150°C, $^{15}N_2$ (single ^{15}N line at −72 ppm) and $^{15}N_2O$ (central N atom at −148 ppm and terminal N atom at −232 ppm) are observed in the ^{15}N NMR spectrum as described above for HZSM-5. The broad ^{15}N line at −364 ppm in Figs. 4b and 4c is assigned to adsorbed methylamine or NH_4^+ (38). The broadening is a result of an interaction with paramagnetic Cu^{2+} since copper is known to strongly bind nitrogen ligands. The ^{15}N line at −98 ppm of Fig. 4c is assigned to *N*-methyl-2-propanimine. The ^{15}N NMR peak of *N*-methyl-2-propanimine observed during the decomposition of acetone [^{15}N]oxime on CuZSM-5 (−98 ppm) is significantly shifted from the peak observed on HZSM-5 (−191 ppm). Protonation of imines is known to produce large shifts in the observed ^{15}N chemical shift values and this may account for the differences in the observed chemical shift values for acetone [^{15}N]oxime and *N*-methyl-2-[^{15}N]propanimine on HZSM-5 and CuZSM-5 (35).

Reactions of Adsorbed Acetone Oxime with NO on HZSM-5 and on CuZSM-5

The ^{15}N MAS NMR spectra of preadsorbed acetone [^{15}N]oxime with ^{14}NO and adsorbed acetone [^{14}N]oxime with ^{15}NO on HZSM-5 and on CuZSM-5 are shown in Figs. 5 and 6. The ^{15}N peak at ∼−148 ppm in Fig. 5a is due to adsorbed acetone [^{15}N]oxime on HZSM-5, and the ^{15}N peak at −102 ppm in Fig. 6a is due to the adsorbed acetone [^{15}N]oxime on CuZSM-5 as discussed in the last section. Three main reaction products, N_2 (−72 ppm), N_2O (central N at −148 ppm and terminal N at −232 to −235 ppm), and $^{15}NH_3CH_2$ or NH_4^+ (at ∼−363 ppm), are observed in the ^{15}N NMR spectrum when acetone [^{15}N]oxime and NO react on CuZSM-5 and HZSM-5 (35, 37, 39). For the samples of adsorbed acetone oxime and ^{15}NO (Figs. 5d–5f and 6d–6f), N_2 and N_2O are produced at room temperature on CuZSM-5, but not until ∼150°C on HZSM-5. The peak at −362 to −364 ppm in Figs. 5c and 6c is assigned to adsorbed methylamine or NH_4^+. The relative intensities of the two nitrogen peaks at −148 and −235 assigned to N_2O vary depending on whether the acetone oxime or the NO is ^{15}N-labeled. In Fig. 6e, the ratio of the relative integrated areas of the peaks at −148 and −235 ppm was 3 : 1, and in Fig. 6b, the ratio of the relative integrated areas of the peaks at −148 and −235 ppm was 1 : 3. These results show that when ^{15}NO reacts with acetone [^{14}N]oxime on CuZSM-5 (Fig. 6e), the product N_2O contains the ^{15}N label on the central nitrogen three times more often than on the terminal nitrogen. Similarly, when ^{14}NO reacts with acetone [^{15}N]oxime on CuZSM-5 (Fig. 6e), the product N_2O contains the ^{15}N label on the terminal nitrogen three times more often than on the central nitrogen. The implications of the different intensities of the N_2O ^{15}N NMR peaks are presented in the Discussion.

The overall integrated ^{15}N signal intensities for the spectra shown in Figs. 2c, 4c, 5c, and 6c vary by less than 10%. This variation is most likely due to small differences in the amounts of acetone oxime adsorbed on the zeolites and the variation in the position of sealed samples loaded in the NMR rotor for each measurement.

The ^{13}C NMR spectra (not shown) of ^{14}NO and preadsorbed acetone [2-^{13}C]oxime on HZSM-5 and on CuZSM-5 heated to various temperatures are similar to the ^{13}C NMR spectra for the reaction of acetone [2-^{13}C]oxime on HZSM-5 and on CuZSM-5 recorded in the absence of NO. One difference is a ^{13}C NMR peak at 55 ppm that is observed after heating acetone [2-^{13}C]oxime on HZSM-5 to 200°C. This peak at 55 ppm is assigned to methanol. In ^{13}C single-pulse excitation spectra of acetone [2-^{13}C]oxime on HZSM-5 heated to 350°C, a ^{13}C NMR peak at 182 ppm was observed and is assigned to CO.

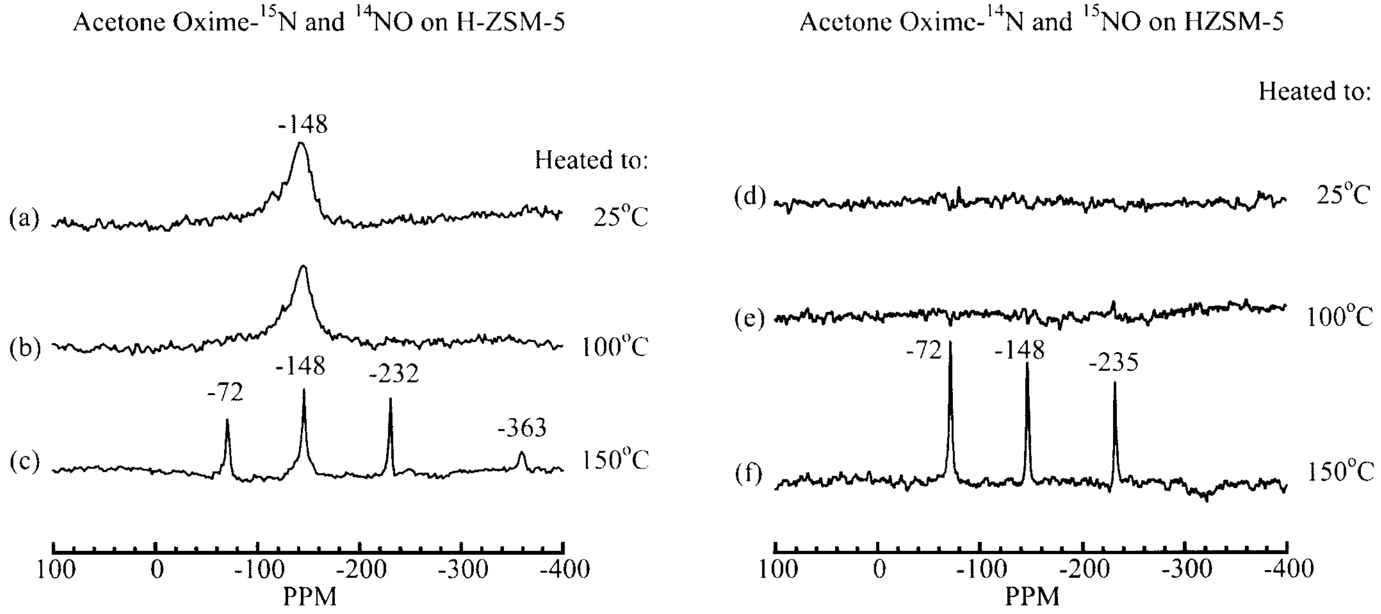

FIG. 5. ^{15}N MAS NMR spectra of adsorbed acetone oxime and NO on HZSM-5. The ^{15}N spectra of acetone [^{15}N]oxime and ^{14}NO on the left (a–c), were acquired at room temperature after the sealed sample was heated to the indicated temperatures. The spectra of acetone [^{14}N]oxime and ^{15}NO, on the right (d–f), were acquired at room temperature after the sealed sample was heated to the indicated temperatures. NS (number of scans acquired) was (a) 5800, (b) 5600, (c) 9200, (d) 12,000, (e) 15,400, and (f) 20,000.

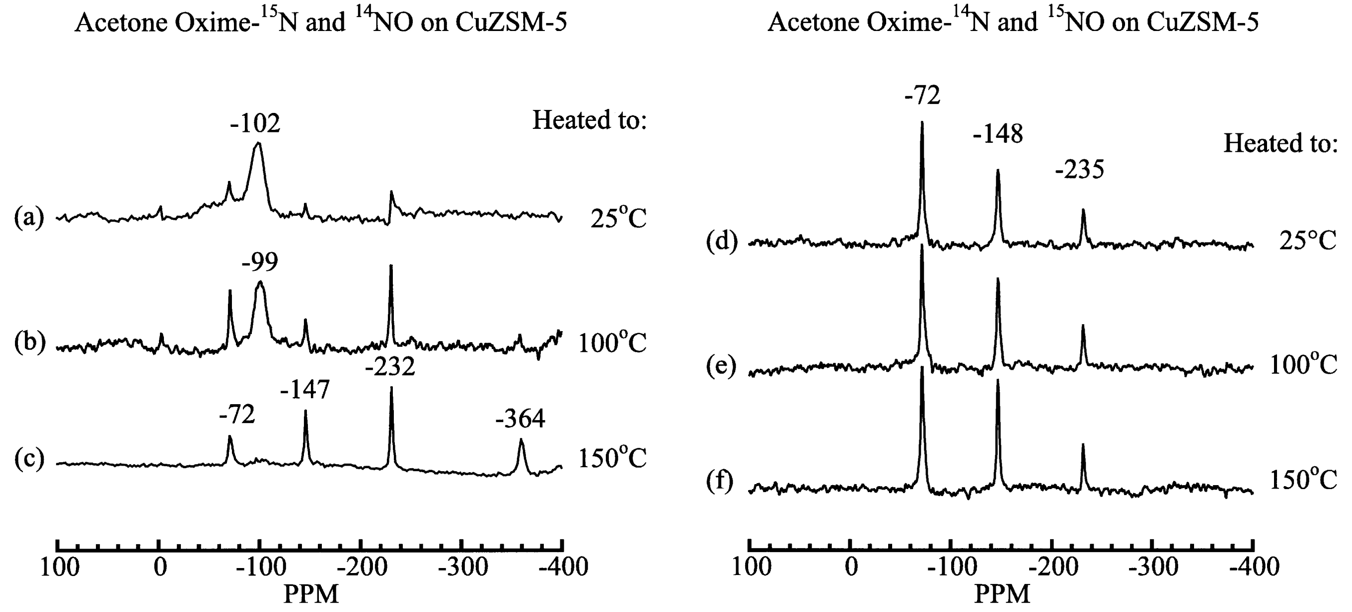

FIG. 6. ^{15}N MAS NMR spectra of adsorbed acetone oxime and NO on CuZSM-5. The spectra of acetone [^{15}N]oxime and ^{14}NO on the left (a–c), were acquired at room temperature after the sealed sample was heated to the indicated temperatures. The spectra of acetone [^{14}N]oxime and ^{15}NO, on the right (d–f), were acquired at room temperature after the sealed sample was heated to the indicated temperatures. NS (number of scans acquired) was (a) 21,500, (b) 8500, (c) 6000, (d) 21,000, (e) 20,000, and (f) 20,000.

Reactions of the Adsorbed Hydrolysis Products of Acetone Oxime with NO

The reaction of various hydrolysis products of acetone oxime with NO on HZSM-5 and CuZSM-5 are presented in Fig. 7. Three main reaction products, N_2 (a single line at ca. −72 ppm), N_2O (central N at ca. −148 ppm and terminal N at ca. −232 ppm), and NH_4^+ or CH_3NH_2 (−364 ppm), were observed in the spectra (Fig. 7). This suggests that the hydrolysis products of acetone oxime (as well as acetone oxime itself) react with NO to form N_2, N_2O, CH_3NH_2, and/or NH_4^+.

The ^{15}N MAS NMR spectra of adsorbed $H_2{}^{15}NOH \cdot HCl$ adsorbed on HZSM-5 and on CuZSM-5, and adsorbed $CH_3{}^{15}NH_2 \cdot HCl$ adsorbed on HZSM-5, all with ^{14}NO after heating to 150°C are presented in Figs. 7a–7c. [^{15}N]Methylamine on HZSM-5 reacts with NO to form nitrogen as indicated by the peak at −72 ppm in Fig. 7a. The peak at −364 ppm in Fig. 7a is due to the unreacted [^{15}N]methylamine adsorbed on HZSM-5. [^{15}N]Hydroxylamine on HZSM-5 reacted with NO at 150°C (Fig. 7b) to form N_2O (peaks at −147 and −232 ppm) and NH_4^+ (peak at −364 ppm) (38). The relative intensities of the two N_2O peaks are approximately equal. When [^{15}N]hydroxylamine was adsorbed on CuZSM-5, the sample turned green, indicating a strong interaction between the nitrogen of hydroxylamine and copper in ZSM-5. [^{15}N]Hydroxylamine on CuZSM-5 (Fig. 7c) reacted with NO at 150°C to form N_2O (peaks at −147 and 232 ppm) and N_2 (peak at −72 ppm). Again, the relative intensities of the two N_2O peaks are approximately equal, suggesting that the label appears equally on the central and terminal nitrogen atoms in N_2O.

The ^{15}N MAS NMR spectra showing the reaction of adsorbed adsorbed acetone on CuZSM-5, $H_2{}^{14}NOH \cdot HCl$ on CuZSM-5 and on HZSM-5, adsorbed $CH_3{}^{14}NH_2 \cdot HCl$ on HZSM-5 all with ^{15}NO after heating to 150°C are presented in Figs. 7d–7g. Since acetone is the major hydrolysis product of acetone oxime adsorbed on CuZSM-5, we examined the products formed when acetone and ^{15}NO react on CuZSM-5 at 150°C (Fig. 7d). The products of the reaction of acetone and ^{15}NO on CuZSM-5 at 150°C are N_2O (peaks at −147 and −232 ppm) and CH_3NH_2 or NH_4^+ (peak at −364 ppm). In Fig. 7e, the reaction of methylamine adsorbed on HZSM-5 and ^{15}NO at 150°C produces N_2 (peak at −72 ppm) and N_2O (peaks at −147 and −232 ppm). Since N_2O is not observed when [^{15}N]methylamine and NO react on HZSM-5 at 150°C, the disproportionation of ^{15}NO on HZSM-5 is thought to be responsible for the formation of N_2O. This result was confirmed in a separate experiment by the direct observation of ^{15}NO disproportionation on HZSM-5. When hydroxylamine reacts with ^{15}NO at 150°C on HZSM-5 (Fig. 7f) and CuZSM-5 (Fig. 7g), N_2O is produced on both CuZSM-5 and HZSM-5 as indicated by the peaks at −147 and −232 ppm and N_2 is formed on CuZSM-5 as indicated by the peak at −72 ppm.

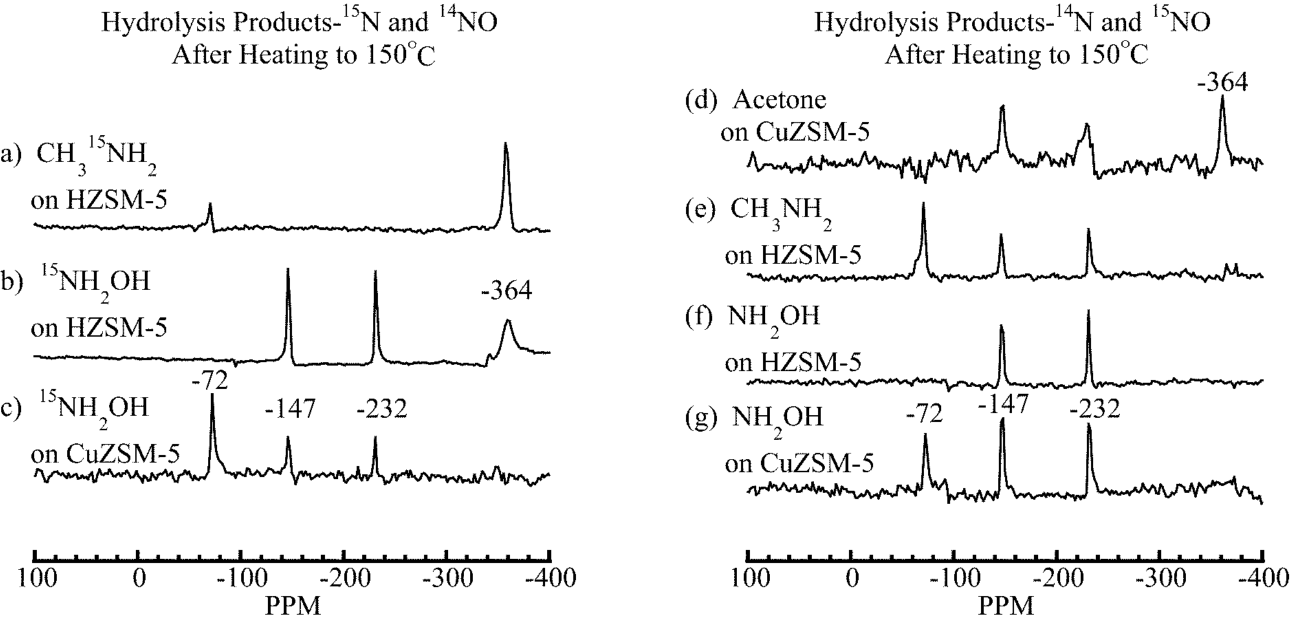

FIG. 7. ^{15}N MAS NMR spectra of the hydrolysis products of acetone oxime with NO on CuZSM-5 and HZSM-5 after heating to 150°C. All spectra were acquired at room temperature. On the left (a–c), are the spectra of the ^{15}N-labeled hydrolysis products with ^{14}NO on HZSM-5—after heating the sealed samples to 150°C: (a) $CH_3{}^{15}NH_2 \cdot HCl$ on HZSM-5 + ^{14}NO, (b) $H_2{}^{15}NOH \cdot HCl$ on HZSM-5 + ^{14}NO, (c) $H_2{}^{15}NOH \cdot HCl$ on CuZSM-5 + ^{14}NO. On the right (d–g), the ^{15}N MAS NMR spectra of the ^{14}N-labeled hydrolysis products + ^{15}NO—after heating to 150°C are shown: (d) acetone on CuZSM-5 + ^{15}NO, (e) $CH_3{}^{14}NH_2 \cdot HCl$ on HZSM-5 + ^{15}NO, (f) $H_2{}^{14}NOH \cdot HCl + {}^{15}NO$ on HZSM-5 + NO, (g) $H_2NOH \cdot HCl$ on CuZSM-5 + ^{15}NO. NS (number of scans acquired) was (a) 6000, (b) 11,000, (c) 20,000, (d) 12,000, (e) 20,000, (f) 12,000, and (g) 20,000.

DISCUSSION

Adsorption of Acetone Oxime on HZSM-5 and on CuZSM-5

The ^{13}C chemical shift for the C-2 carbon of solid, synthesized acetone [2-^{13}C]oxime was measured to be 156 ppm (vs TMS) (spectrum not shown here). However, the ^{13}C chemical shifts of adsorbed acetone [2-^{13}C]oxime on HZSM-5 and CuZSM-5 at 1 : 1 coverage were shifted downfield to 172 and 166 ppm, respectively, and were coverage-dependent. The shift of the C-13 NMR peak of acetone [2-^{13}C]oxime on adsorption in the zeolites relative to "free" solid acetone oxime is evidence of an interaction with the zeolite. Because of spin diffusion and averaging at high coverage, the ^{13}C NMR shift from the pure solid for the 8 : 1 coverage is much smaller in magnitude than for the 1 : 1 coverage. A similar coverage dependence has been observed for acetone adsorbed on various zeolites (33, 34, 40). The interpretation from this earlier work was that the ^{13}C chemical shift of acetone depends on the degree of protonation of the carbonyl group of the adsorbed acetone, in other words on the acidity of the support. The ^{15}N chemical shift for solid, synthesized acetone [^{15}N]oxime was measured to be −55 ppm (vs $CH_3{}^{15}NO_2$). The ^{15}N NMR peaks from acetone [^{15}N]oxime absorbed on HZSM-5 and on CuZSM-5 were shifted upfield to −148 and −102 ppm, respectively. The large upfield shifts from the ^{15}N chemical shift values for solid acetone oxime on adsorption also suggest protonation of the acetone oxime. The ^{15}N chemical shifts of imines have been shown to be very sensitive to protonation by NMR studies of imines in different solvents and adsorbed on zeolites (35, 36).

The chemical shifts (^{15}N and ^{13}C) of adsorbed acetone oxime on HZSM-5 and on CuZSM-5 are different, suggesting that the degree of protonation on the two zeolites is different. The ^{15}N and ^{13}C chemical shifts for solid synthesized acetone oxime and acetone oxime adsorbed on CuZSM-5 and HZSM-5 are plotted in Fig. 8. The ^{15}N and ^{13}C chemical shifts for acetone oxime adsorbed on CuZSM-5 lie between the chemical shifts for solid acetone and acetone oxime adsorbed on HZSM-5 and are linearly correlated. This implies that CuZSM-5 contains residual Brønsted acid sites that are weaker than the Brønsted acid sites in HZSM-5, so that the change in chemical shift of acetone oxime adsorbed on CuZSM-5 is smaller than for the more acidic HZSM-5 compared with the solid acetone oxime. Xu *et al.* have previously reported that the chemical shift for adsorbed probe molecules varies with the acidity of the zeolite (33).

It is also possible that the observed variations in chemical shift are due to the presence of the exchanged copper cations rather than the presence of acid sites. Perhaps the

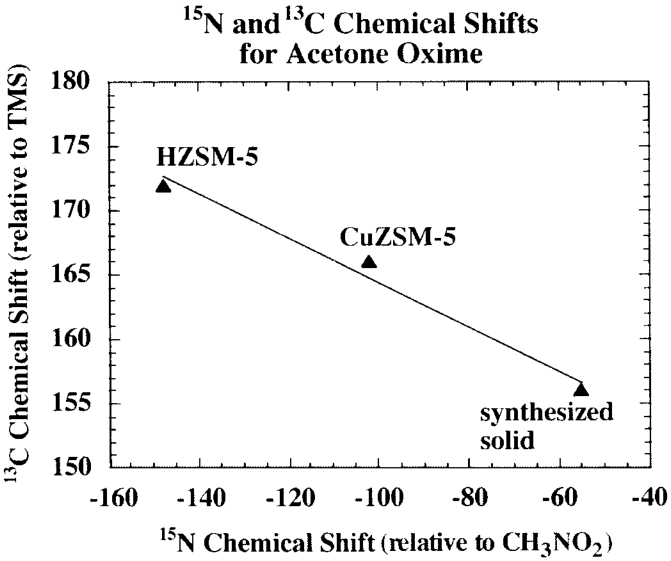

FIG. 8. Plot of ^{15}N and ^{13}C chemical shifts for acetone oxime (acetone [2-^{13}C]oxime and acetone [^{15}N]oxime) adsorbed on CuZSM-5 and HZSM-5 and the solid synthesized acetone oxime (data from Table 2). The acetone oxime coverage was approximately one adsorbate molecule per Brønsted acid or cation site.

acetone oxime interacts with the exchanged copper species. In this study, copper (Cu^{2+}) is ion-exchanged into ZSM-5 from an aqueous solution of a copper salt. Several groups have reported the autoreduction of Cu^{2+} to Cu^{+} after heating CuZSM-5 to 450°C (12, 31). However, the CuZSM-5 samples used in this study have been evacuated only at room temperature and are not rigorously dehydrated or autoreduced. Therefore, it is likely that the copper remains in the 2+ oxidation state over the course of these experiments.

Decomposition of Acetone Oxime Adsorbed on HZSM-5 and on CuZSM-5

Acetone oxime can be hydrolyzed by two different pathways as shown in Scheme 1. Acetone oxime can hydrolyze directly to produce acetone and hydroxylamine (reaction 1A), and/or acetone oxime can rearrange via the Beckman rearrangement to form *N*-methylacetamide (reaction 1B), which further hydrolyzes to produce acetic acid and methylamine (reaction 2) (41). The subsequent reaction of acetone and methylamine, which are the hydrolysis products in reactions 1 and 2, leads to the production of *N*-methyl-2-propanimine (reaction 3). The major products observed by ^{13}C NMR when acetone [2-^{13}C]oxime was decomposed on HZSM-5 were *N*-methylacetamide or acetic acid, and *N*-methyl-2-propanimine. Small amounts of acetone were

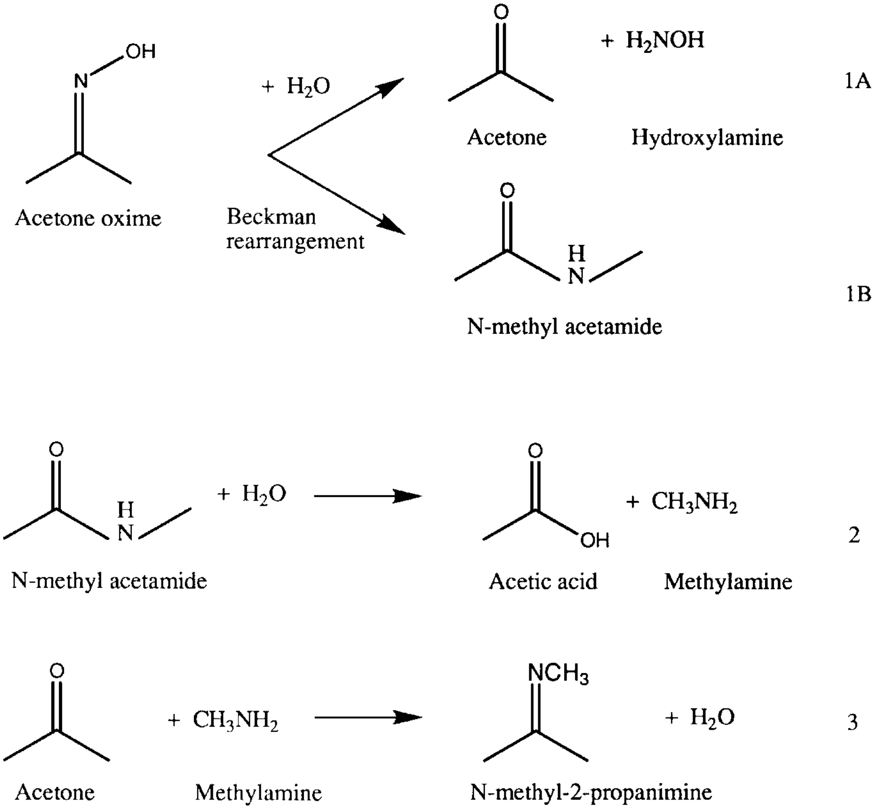

SCHEME 1. Reactions of acetone oxime.

also formed on HZSM-5. Acetone [2-^{13}C]oxime adsorbed on CuZSM-5 decomposed to form acetone as the major product through the direct hydrolysis of acetone oxime as monitored by ^{13}C NMR. Minor products, acetic acid and *N*-methyl-2-propanimine, were also observed in the ^{13}C NMR spectra of acetone [2-^{13}C]oxime on CuZSM-5. In a previous FT-IR/mass spectrometry study, acetone and hydroxylamine were the main hydrolysis products observed during the decomposition of acetone oxime on CuZSM-5 (41). In the same study, minor products, such as *N*-methylacetamide, acetic acid, and methylamine were also detected by FT-IR (41).

NMR peaks (Figs. 1 and 2) were observed at 197 ppm (^{13}C NMR) and −191 ppm (^{15}N NMR) when samples of adsorbed acetone oxime on HZSM-5 were heated to $>150°$C and these resonances have been assigned to *N*-methyl-2-propanimine. The assignment of these resonances to *N*-methyl-2-propanimine is based on two recent ^{13}C MAS NMR studies of the reaction of acetone and amines on HZSM-5 (34, 35). Xu *et al.* observed that acetone and ammonia reacted to form 2-propanimine which has ^{15}N and ^{13}C NMR shifts of −190 and 197 ppm, respectively (35). Biaglow *et al.* observed the formation of 2-propanimine ($\delta_{\text{C-13}} = 199$ ppm) from acetone and NH_3 and the formation of 2,2-*N*-methyl-2-propanimine ($\delta_{\text{C-13}} = 189$ ppm) from dimethylamine and acetone on HZSM-5 (34). These NMR peaks were assigned to the fully or partially protonated forms of the imines. The ^{15}N chemical shifts of imines are very sensitive to protonation and shifts of greater than 100 ppm have been observed for imines in solvents with different acidities (36). The chemical shifts observed in the NMR studies of related imines correspond very well with those observed in our experiments of acetone oxime decomposition on HZSM-5. NMR peaks from acetone oxime decomposition on CuZSM-5 at 190 ppm (^{13}C NMR) and −98 ppm (^{15}N NMR) in Figs. 3 and 4 are therefore assigned to *N*-methyl-2-propanimine. The different ^{15}N chemical shifts found for *N*-methyl-2-propanimine on HZSM-5 and on CuZSM-5 are attributed to differences in the interaction of *N*-methyl-2-propanimine with acid sites and Cu^{2+} cation sites in HZSM-5 and CuZSM-5. Again this could be attributed to hydrogen bonding effects which are known to produce large variations in the NMR chemical shifts of imines (35).

N_2 and N_2O were also detected by ^{15}N MAS NMR (Figs. 2 and 4) when samples of adsorbed acetone [^{15}N]oxime on HZSM-5 and CuZSM-5 were heated to 150°C. Since acetone [^{15}N]oxime is the only source of nitrogen, the gaseous (N_2 and N_2O) products can only be $^{15}N^{15}N$ ($\delta_{\text{N-15}} = -72$ ppm) and $^{15}N^{15}NO$ [$\delta_{\text{N-15}} = -148$ (central N), −232 ppm (terminal N)]. Resonances attributable to hydroxylamine ($\delta_{\text{N-15}} = -298$ ppm) were not observed in the ^{15}N NMR spectra in Figs. 2 and 4. Presumably this is because if any hydroxylamine formed, it reacted to produce N_2O and/or N_2. The ^{15}N NMR peak at −363 ppm in Fig. 2c has been assigned to methylamine. Only a weak and broad peak at −363 ppm is observed in the ^{15}N NMR spectrum of acetone [^{15}N]oxime on CuZSM-5 (Fig. 4c). This is due to a strong interaction between the paramagnetic Cu^{2+} and the amine group of methylamine or hydroxylamine. A color change (blue for methylamine and green for hydroxylamine) was observed when authentic samples of methylamine or hydroxylamine were adsorbed on CuZSM-5, suggesting that the amine group is coordinated to the copper. EPR experiments have been done to verify the coordination of the nitrogen of the amine group to Cu^{2+}.

Reactions of Adsorbed Acetone [^{15}N]Oxime with ^{14}NO

The ^{15}N NMR spectra of acetone [^{15}N]oxime adsorbed on HZSM-5 in the absence of ^{14}NO (Fig. 2c) and in the presence of ^{14}NO (Fig. 5c) indicate that N_2, N_2O, CH_3NH_2, and/or NH_4^+ were formed on both samples after heating to 150°C. Two major differences between the spectra (Figs. 2c and 5c) should be noted. First, in Fig. 2c, an additional peak at −191 ppm due to *N*-methyl-2-propanimine was observed. Second, the peak due to methylamine ($\delta_{\text{N-15}} = -363$ ppm) is larger relative to the other gas-phase peaks in Fig. 2c than in Fig. 5c. The explanation is that the methylamine formed from the hydrolysis of acetone oxime adsorbed on HZSM-5 reacts with NO to form nitrogen as shown in Fig. 7a, while in the absence of NO, the methylamine remains adsorbed on HZSM-5 and then reacts with acetone.

There are two pathways for the formation of N_2 and N_2O when acetone [^{15}N]oxime reacts with NO. One path results from the interaction of an adsorbed [^{15}N]oxime complex (or its hydrolysis products) and gas-phase ^{14}NO to form mixed-labeled N_2 ($^{15}N^{14}N$) and N_2O ($^{15}N^{14}NO$, $^{14}N^{15}NO$). The second path is the decomposition of unreacted, adsorbed acetone [^{15}N]oxime, resulting in doubly labeled $^{15}N_2$ and $^{15}N_2O$ as shown in Fig. 2c. From the NMR results for the reaction of adsorbed acetone [^{15}N]oxime with ^{14}NO, it is difficult to quantify the amount of $^{15}N_2$ versus $^{14}N^{15}N$ or $^{15}N^{14}NO$ versus $^{14}N^{15}NO$ in Fig. 5c. The broadening of the peak at −148 ppm in Fig. 5c suggests that a substantial portion of the peak intensity is due to unreacted adsorbed acetone oxime which is more strongly adsorbed and less mobile than the gas-phase product N_2O. This is a reasonable since nitric oxide was the limiting reagent. This was further confirmed by comparing the peak at −148 ppm in the ^{15}N NMR spectrum of unlabeled acetone oxime and labeled ^{15}NO (Fig. 5f) which is much narrower than the peak formed with adsorbed acetone [^{15}N]oxime present in Fig. 5c and contains no contribution from the unlabeled acetone oxime.

The ^{15}N NMR spectra of acetone [^{15}N]oxime adsorbed on CuZSM-5 and ^{14}NO (Figs. 6a–6c) showed that N_2 and N_2O were formed at 25 and 100°C, and some unreacted acetone [^{15}N]oxime was still present (peak at −102 ppm).

The gaseous products formed at 25 and at 100°C are mixed-labeled $^{14}N^{15}N$, $^{14}N^{15}NO$, and $^{15}N^{14}NO$ resulting from the interaction of adsorbed acetone [^{15}N]oxime and gas-phase ^{14}NO as previously observed by Beutel *et al.* (41). The doubly labeled products, $^{15}N_2$ and $^{15}N_2O$, were ruled out as possible products because the formation of these products from adsorbed acetone [^{15}N]oxime did not occur until the sample was heated to 150°C and above (Fig. 4c). The data demonstrate that the interaction of adsorbed acetone [^{15}N]oxime and/or its ^{15}N-labeled hydrolysis products with ^{14}NO results in the formation of a new ^{15}N–^{14}N bond. The reaction of acetone oxime with NO to form N_2 and N_2O occurs at room temperature on CuZSM-5. It should be noted from the ^{15}NMR spectra (Figs. 6b and 6c) that the ratio of the integrated areas of the ^{15}N NMR peaks for $^{15}N^{14}NO$ over $^{14}N^{15}NO$ is $\sim$3 when acetone [^{15}N]oxime is reacted with ^{14}NO. These results are consistent with the study of Beutel *et al.*, who observed mixed-labeled $^{14}N^{15}N$, $^{14}N^{15}NO$, and $^{15}N^{14}NO$ by FT-IR/mass spectrometry studies (41). However, they were not able to quantify the ratio of $^{15}N^{14}NO$ to $^{14}N^{15}NO$ since $^{14}N^{15}NO$ and $^{15}N^{14}NO$ could not be distinguished by mass spectrometry. Using ^{15}N NMR we were able to easily distinguish $^{14}N^{15}NO$ and $^{15}N^{14}NO$ because the inequivalent nitrogen atoms possess different chemical shifts.

Reactions of Adsorbed Acetone [^{14}N]Oxime with ^{15}NO

To simplify the ^{15}N NMR identification of N_2 and N_2O as singly or doubly labeled, reactions of adsorbed acetone [^{14}N]oxime in the presence of ^{15}NO were conducted. This experiment eliminated the ^{15}N doubly labeled products from the direct decomposition of acetone [^{15}N]oxime into $^{15}N_2$ and $^{15}N_2O$. ^{15}N MAS NMR showed that N_2 and N_2O were produced when a sealed sample of ^{15}NO and adsorbed acetone [^{14}N]oxime on HZSM-5 was heated to 150°C (Fig. 5f). No products were detected by ^{15}N NMR below that temperature. Previously, ^{15}NO alone on HZSM-5 produced N_2 and N_2O even at room temperature (39), suggesting that the active sites of HZSM-5 are blocked by adsorbed acetone [^{14}N]oxime in our experiments since no products are detected below 150°C. Therefore, N_2 and N_2O observed at 150°C were not from the ^{15}NO disproportionation reaction and were not from the decomposition of adsorbed acetone oxime either, since the adsorbed acetone oxime is not ^{15}N-labeled. The remaining option is that the N_2 and N_2O observed at 150°C on HZSM-5 resulted from the interaction of adsorbed acetone [^{14}N]oxime and/or its ^{14}N-labeled hydrolysis products with ^{15}NO. The products should be mixed-labeled $^{14}N^{15}N$, $^{14}N^{15}NO$, and $^{15}N^{14}NO$.

A sealed sample of ^{15}NO and adsorbed acetone [^{14}N]oxime on CuZSM-5 showed the formation of N_2 and N_2O at 25°C (Figs. 6d–6f). The spectrum did not change when the sample was heated to 100 and 150°C. Just as on HZSM-5, the decomposition products from adsorbed acetone [^{14}N]oxime cannot be detected by ^{15}N NMR since the adsorbed acetone oxime is not ^{15}N labeled. The N_2 and N_2O observed were not from the ^{15}NO disproportionation either as confirmed in a separate experiment of ^{15}NO disproportionation on CuZSM-5. It is the reaction of adsorbed acetone [^{14}N]oxime and/or its ^{14}N-labeled hydrolysis products with ^{15}NO that results in the formation of mixed-labeled N_2 ($^{14}N^{15}N$) and N_2O ($^{14}N^{15}NO$ and $^{15}N^{14}NO$) as previously observed by Beutel *et al.* (41). The observed partitioning between $^{14}N^{15}NO$ and $^{15}N^{14}NO$ is approximately 3 : 1. Comparison of Figs. 6b and 6e illustrates that the opposite partition is obtained when the isotopic labeling is reversed and acetone [^{15}N]oxime and ^{14}NO react on CuZSM-5. This suggests that the nitrogen–oxygen bond of ^{15}NO remains intact when it reacts with adsorbed acetone [^{14}N]oxime to preferentially form $^{14}N^{15}NO$. The fact that some $^{15}N^{14}NO$ is also formed implies that there is a second route for the production of N_2O when adsorbed acetone [^{14}N]oxime and ^{15}NO react on CuZSM-5. The second route is likely to be the reaction of the hydrolysis products of acetone oxime reacting with ^{15}NO. For example, hydroxylamine adsorbed on CuZSM-5 reacted with ^{15}NO (Fig. 7g) to give N_2 and N_2O, and the two peaks of N_2O were of equal intensity, suggesting no preference for the position of the label.

Reactions of Adsorbed Hydrolysis Products of Acetone Oxime with NO

To clarify the source of gas-phase N_2 and N_2O products, the interaction of the hydrolysis products of acetone oxime with gas-phase NO has been investigated. Since hydroxylamine, acetone, and methylamine were formed during the hydrolysis of acetone oxime on CuZSM-5 and HZSM-5, authentic samples of these hydrolysis products were adsorbed on CuZSM-5 and HZSM-5. [^{15}N]Hydroxylamine, one of the minor hydrolysis products formed on HZSM-5, reacted with-gas phase ^{14}NO to form N_2O with very little production of N_2. Isotopic labeling studies showed that approximately equal amounts of $^{15}N^{14}NO$ and $^{14}N^{15}NO$ and some $^{15}NH_4^+$ were formed (Fig. 7b) due to the reaction of adsorbed [^{15}N]hydroxylamine on HZSM-5 with ^{14}NO starting at room temperature. This observation implies the formation of a ^{14}N–^{15}N bond between $^{15}NH_2OH$ and NO on HZSM-5. The broadening of the peak at -364 ppm (which is assigned to NH_4^+) suggests strong bonding to the zeolite. When [^{15}N]hydroxylamine reacts with ^{14}NO on CuZSM-5, both N_2 and N_2O are formed (Fig. 7c), starting at room temperature. The integrated areas of the two N_2O peaks are approximately equal, suggesting equal amounts of $^{15}N^{14}NO$ and $^{14}N^{15}NO$ are formed.

Equal amounts of $^{14}N^{15}NO$ and $^{15}N^{14}NO$ were also observed after reaction at 100°C and above for a sealed sample of [^{14}N]hydroxylamine adsorbed on HZSM-5 in the presence of ^{15}NO (Fig. 7f). With the same adsorbates on CuZSM-5, approximately equal amounts of $^{14}N^{15}NO$ and $^{15}N^{14}NO$ were observed starting at room temperature, but a measurable amount of N_2 ($^{14}N^{15}N$) was not detected until ~150°C (Fig. 7g). These isotopic labeling experiments clearly show that the hydrolysis product, hydroxylamine, reacts easily with NO to form a new N–N bond, on both catalysts, with two N atoms from two different sources: one N from adsorbed hydroxylamine and the other N from gaseous NO, without preference. Beutel *et al.* observed the formation of mixed-labeled N_2 and N_2O when hydroxylamine and NO reacted on CuZSM-5, but they could not distinguish the $^{14}N^{15}NO$ and $^{15}N^{14}NO$ (41).

Methylamine, the primary hydrolysis product of acetone oxime on HZSM-5, reacted with gas-phase NO to form nitrogen. The authentic sample of [^{15}N]methylamine · HCl adsorbed on HZSM-5 in the presence of ^{14}NO resulted in two NMR peaks due to the formation of nitrogen (−72 ppm) and unreacted methylamine (−363 ppm) after heating to 150°C (Fig. 7a). The authentic sample of [^{14}N]methylamine · HCl on HZSM-5 reacted with ^{15}NO to form both N_2 and N_2O (Fig. 7e). The N_2O results from the disproportionation of ^{15}NO on HZSM-5, since no N_2O was observed when methylamine reacts with unlabeled NO.

Since acetone is the major hydrolysis product of acetone oxime on CuZSM-5, the reaction of acetone with NO was also studied (Fig. 7d). The sealed sample containing the adsorbed acetone on CuZSM-5 and ^{15}NO showed the formation of N_2O starting at room temperature. After heating to 150°C and subsequently cooling to room temperature for the NMR spectrum, a new peak at −364 ppm emerged, and this peak was assigned to CH_3NH_2 or NH_4^+.

Implications of these Results for the Mechanism for SCR of NO_x by Propane

Solid-state NMR has proven to be a valuable tool for studying the reactions of acetone oxime, a proposed intermediate for the SCR of NO_x with propane on CuZSM-5 and HZSM-5. In the absence of NO, acetone oxime decomposes primarily to acetone, hydroxylamine, nitrogen, and nitrous oxide on CuZSM-5 and acetic acid, methylamine, nitrogen, and nitrous oxide on HZSM-5. The different products observed on the two zeolites reflect differences in the Brønsted acid sites and in the cation sites present in HZSM-5 and CuZSM-5. The reactivity of acetone oxime adsorbed on HZSM-5 is a result of the acid-catalyzed Beckman rearrangement of acetone oxime to *N*-methylacetamide which subsequently hydrolyzes to acetic acid and methylamine (Scheme 1). The reactivity of CuZSM-5, which has a smaller number of acid sites, is governed by the direct hydrolysis of acetone oxime to acetone and hydroxylamine. On both CuZSM-5 and HZSM-5, nitrogen and nitrous oxide are formed from adsorbed acetone oxime after heating to ~150°C presumably from reaction of acetone oxime and its nitrogen-containing hydrolysis products, such as methylamine and hydroxylamine.

The NMR studies were conducted under conditions of thermodynamic equilibrium and at temperatures substantially below the relevant catalytic temperatures of ~400°C. Therefore, information about the catalytic mechanism cannot be directly determined from the NMR results. Acetone oxime and NO on CuZSM-5 and HZSM-5 react to form nitrogen, nitrous oxide, and NH_4^+ or methylamine. Reaction of a nitrogen-containing surface species with NO to form N_2 has previously been suggested by a number of researchers as a crucial element of the SCR mechanism (10, 12, 15, 20, 22, 23, 41). Nitrogen and nitrous oxide are formed at room temperature on CuZSM-5, but not until 150°C on HZSM-5, suggesting that the reaction of acetone oxime and NO to form nitrogen and nitrous oxide on CuZSM-5 is more facile than the reaction of acetone oxime and NO on HZSM-5.

The NMR results from the reaction of acetone oxime with ^{15}NO on CuZSM-5 to form N_2O demonstrate that the ^{15}NO bond (of gas phase NO) remains intact when it reacts with acetone oxime as evidenced by the NMR peak intensities of the product N_2O. This result is consistent with the mechanism proposed by Adelman *et al.* (23) for NO_x reduction of propane over CuZSM-5. Their mechanism suggests that acetone oxime reacts with NO to form an intermediate that further decomposes to N_2O and an oxygenated hydrocarbon species. Li and Armor have observed the decomposition of N_2O to N_2 on transition metal-exchanged zeolites and, in particular, on CuZSM-5 under SCR reaction conditions (42). Rebrov *et al.* observed N_2O on low-loaded CuZSM-5 catalysts under SCR reaction conditions (21). The final step of the mechanism shows further reaction of the oxygenated intermediate and N_2O to form nitrogen, acetone, and water (23). The NMR results presented in this paper support the previously proposed intermediacy of acetone oxime in the SCR of NO_x by propane and provide additional details about the reactions of acetone oxime on HZSM-5 and CuZSM-5 under conditions of thermodynamic equilibrium.

CONCLUSIONS

Solid-state NMR was used to investigate the reactions of acetone oxime adsorbed on CuZSM-5 and on HZSM-5. The decomposition of isotopically labeled acetone oxime on HZSM-5 and on CuZSM-5 was monitored using ^{15}N and ^{13}C NMR. The predominant reaction path for acetone oxime was different on HZSM-5 and on CuZSM-5. The differences are attributed to an enhancement of acid chemistry on HZSM-5 which leads to the formation of acetic acid and methylamine by acid-catalyzed reactions. On CuZSM-5, acetone oxime decomposes primarily to acetone and hydroxylamine. Acetone oxime and its hydrolysis products further react to form N_2 and N_2O on both zeolites. Acetone oxime reacts with gas-phase NO on HZSM-5 and on CuZSM-5 to form a new N–N bond. The nitrogen comes from two different sources: one from the adsorbed oxime complex and the other from gas-phase NO. The ^{15}N NMR results show that the NO bond of gas-phase NO remains intact when it reacts with adsorbed acetone oxime to form N_2O. The reaction of acetone oxime and NO to form N_2 and N_2O proceeds at room temperature on CuZSM-5, but not until 150°C on HZSM-5.

^{15}N NMR has provided important information, such as the identification and quantification of $^{15}N^{14}NO$ and $^{14}N^{15}NO$, which are not distinguished in mass spectrometry. In addition, NMR was used to determine the partition between $^{14}N^{15}NO$ and $^{15}N^{14}NO$ in product N_2O. The results demonstrate the potential of solid-state NMR for studying surface species that may be important catalytic intermediates.

ACKNOWLEDGMENTS

Acknowledgment is made to the University of Iowa and to the donors of the Petroleum Research Fund, administered by the American Chemical Society, for funding of this research. Dr. Russell Larsen is acknowledged for assistance with experiments and helpful discussions. Professor John Wiencek is acknowledged for use of his ICP/AES instrument.

REFERENCES

1. Bosch, H., Janssen, F., *Catal. Today* **2**, 369 (1987).
2. Iwamoto, M., Yahiro, H., Shundo, Y., Yu-u, Y., Misonu, N., *Shokubai* **32**, 430 (1990).
3. Held, W., Konig, A., Richter, T., and Pupper, L., *SAE Paper* **900**, 469 (1990).
4. Shelef, M., *Chem. Rev.* **95**, 209 (1995).
5. Cho, B. K., *J. Catal.* **142**, 418 (1993).
6. Li, Y., and Armor, J. N., *Appl. Catal. B* **1**, L3 (1991).
7. Li, Y., and Armor, J. N., *Appl. Catal. B* **3**, 239 (1994).
8. Burch, R., and Scire, S., *Appl. Catal. B* **3**, 295 (1994).
9. Feng, X., and Hall, W. K., *J. Catal.* **166**, 368 (1997).
10. Beutel, T., Adelman, B., and Sachtler, W. M. H., *Catal. Lett.* **37**, 125 (1996).
11. Li, Y., Slager, T. L., and Armor, J. N., *J. Catal.* **150**, 338 (1994).
12. Witzel, F., Sill, G. A., and Hall, W. K., *J. Catal.* **149**, 229 (1994).
13. d'Itri, J. L., and Sachtler, W. M. H., *Appl. Catal. B* **2**, L7 (1993).
14. Montreuil, C. N., and Shelef, M., *Appl. Catal. B* **1**, L1 (1992).
15. Halasz, I., Brenner, A., Ng, K. Y. S., and Hou, Y., *J. Catal.* **161**, 359 (1996).
16. Ukiso, Y., Sato, S., Abe, A., and Yoshida, K., *Appl. Catal. B* **2**, 147 (1993).
17. Sadykov, V. A., Baron, S. L., Matyshak, V. A., Alikina, G. M., Bunina, R. V., Rozovskii, A. Ya., Lunin, V. V., Lunina, E. V., Kharlanov, A. N., Ivanova, A. S., and Veniaminov, S. A., *Catal. Lett.* **37**, 157 (1996).
18. Adelman, B. J., Beutel, T., Lei, G.-D., and Sachtler, W. M. H., *J. Catal.* **158**, 327 (1996).
19. Smits, R. H. H., and Iwasawa, Y., *Appl. Catal. B* **6**, L201 (1995).
20. Yokoyama, C., and Misono, M., *J. Catal.* **150**, 9 (1994).
21. Rebrov, E. V., Simakov, A. V., Sazonova, N. N., Rogov, V. A., and Barannik, G. B., *Catal. Lett.* **51**, 27 (1998).
22. Kharas, K. C. C., *Appl. Catal. B Environ.* **2**, 207 (1993).
23. Adelman, B. J., Beutel, T., Lei, G.-D., and Sachtler, W. M. H., *Appl. Catal. B* **11**, L1 (1996).
24. Cowan, A. D., Dumpelmann, R., and Cant, N. W., *J. Catal.* **151**, 356 (1995).
25. Barton, D., and Ollis, W. D., *in* "Comprehensive Organic Chemistry: The Synthesis and Reactions of Organic Compounds" (J. L. Sutherland, Ed.), Vol. 2, p. 391 (1979).
26. Haw, J. F., *in* "NMR Techniques in Catalysis" (A. T. Bell and A. Pines, Eds.), pp. 139–194 (1994).
27. Slichter, C. P., *Annu. Rev. Phys. Chem.* **37**, 25 (1986).
28. Duncan, T. M., *Colloids Surf.* **45**, 11 (1990).
29. Narita, E., Sato, K., Yatabe, N., and Okabe, T., *Ind. Eng. Chem. Prod. Res. Dev.* **24**, 507 (1985).
30. Shiralkar, V. P., and Clearfield, A., *Zeolites* **9**, 363 (1989).
31. Larsen, S. C., Aylor, A., Bell, A. T., and Reimer, J. A., *J. Phys. Chem.* **98**, 11533 (1994).
32. Semon, W. L., "Organic Synthesis," Coll. Vol. 1, p. 318 (1941).
33. Xu, T., Munson, E. J., and Haw, J. F., *J. Am. Chem. Soc.* **116**, 1962 (1994).
34. Biaglow, A. I., Sepa, J., Gorte, R. J., and White, D., *J. Catal.* **151**, 373 (1995).
35. Xu, T., Zhang, J., and Haw, J. F., *J. Am. Chem. Soc.* **117**, 3171 (1995).
36. Allen, M., and Roberts, J. D., *J. Org. Chem.* **45**, 130 (1980).
37. Mastikhin, V. M., Mudrakovsky, I. L., and Filimonova, S. V., *Chem. Phys. Lett.* 175 (1988).
38. Michel, D., Germanus, A., and Pfeifer, H., *J. Chem. Soc. Faraday Trans.* **78**, 237 (1982).
39. Mastikhin, V. M., and Filimonova, S. V., *J. Chem. Soc. Faraday Trans.* **88**, 1473 (1992).
40. Biaglow, A. I., Gorte, R. J., Kokotailo, G. T., and White, D., *J. Catal.* **148**, 779 (1994).
41. Beutel, T., Adelman, B. J., Lei, and Sachtler, W. M. H., *Catal. Lett.* **32**, 83 (1995).
42. Li, Y., and Armor, J., *Appl. Catal. B Environ.* **3**, 55 (1993).